



## Note

## $\delta^{34}\text{S}$ character of organosulfur compounds in kerogen and bitumen fractions of sedimentary rocks



Hendrik Grotheer<sup>a,\*</sup>, Paul F. Greenwood<sup>a,b</sup>, Malcolm T. McCulloch<sup>b</sup>, Michael E. Böttcher<sup>c</sup>, Kliti Grice<sup>a</sup>

<sup>a</sup> WA-OIGC, Department of Chemistry, The Institute for Geoscience Research, Curtin University, GPO Box U1987, Perth, WA 6845, Australia

<sup>b</sup> School of Earth and Environment, University of Western Australia, Crawley, WA 6009, Australia

<sup>c</sup> Geochemistry and Stable Isotope Biogeochemistry Group, Leibniz Institute for Baltic Sea Research (IOW), D-18119 Warnemünde, Germany

## ARTICLE INFO

## Article history:

Received 2 January 2017

Received in revised form 18 April 2017

Accepted 19 April 2017

Available online 18 May 2017

## Keywords:

Organosulfur compounds

Stable sulfur isotopes

Kerogen

Bitumen

HyPy

Hydropyrolysis

## ABSTRACT

Hydropyrolysis (HyPy) of S-containing oil mature rock samples from two geologic settings each produced much higher concentrations of organosulfur compounds (OSCs) compared to their free occurrence in the bitumen. The  $\delta^{34}\text{S}$  values of the most abundant OSCs from the kerogen and in the bitumen, were measured by gas chromatography inductively coupled plasma mass spectrometry (GC-ICP-MS). DBT and mDBTs from the HyPy processed kerogen fractions showed a distinct  $^{34}\text{S}$  depletion, with  $\delta^{34}\text{S}$  values up to 12‰ lighter than their bitumen occurrence. The different  $\delta^{34}\text{S}$  values of OSCs from the kerogen and bitumen fractions is likely reflective of differences in timing of production, reduced sulfur sources or organic sulfurisation mechanism.

© 2017 Elsevier Ltd. All rights reserved.

### 1. Introduction

The emerging capability of compound specific S isotope analysis (CS-S-IA; Amrani et al., 2009; Greenwood et al., 2014) presents an opportunity to gain a much better understanding of the organic S-cycle and the nature of different S-pools in the Earth's system and may help distinguish different pathways of organic sulfurisation. The distributions and  $\delta^{34}\text{S}$  character of different sedimentary S-pools has helped identify pathways of organic sulfurisation (e.g. Sinninghe Damste and de Leeuw, 1990; Raven et al., 2015). Compound specific  $\delta^{34}\text{S}$  data is also attractive for being free of any inorganic S contribution, which can be problematic for bulk  $\delta^{34}\text{S}$  analysis of sedimentary rocks or fractions due to difficulties in exhaustively removing all pyrite (Cai et al., 2009). Paleoenvironmental reconstructions using compound specific  $\delta^{34}\text{S}$  of OSCs in sedimentary rocks requires knowledge about timing of organic matter (OM) deposition and its sulfurisation, the identity and  $\delta^{34}\text{S}$  values of primary S-sources and the molecular and  $\delta^{34}\text{S}$  fractionation of OSCs during diagenesis and thermal maturation. We measured the  $\delta^{34}\text{S}$  values of OSCs generated from kerogens by hydropyrolysis (HyPy) treatment and compared them to free OSCs

in the corresponding bitumen fractions for several different aged sediments from two geological settings. HyPy has been shown to release indigenous covalently bound hydrocarbons from the kerogen matrix of rock samples (e.g. Love et al., 1995).

### 2. Material and methods

Four Permian or Triassic shales recovered from the Hovea-3 well (Perth Basin, Western Australia; e.g., Thomas et al., 2004; Dawson et al., 2005) and calcareous shale samples from three separate wells of the Lower Cretaceous Toolebuc Formation (Queensland, Australia; Boreham and Powell, 1987; Woltering et al., 2016) were selected for this study. The Toolebuc rocks were much richer in organic matter and generally had slightly higher total sulfur (TS) content (Table 1). All samples had thermal maturities within the oil window (Table 1;  $R_c = 0.7 - 0.8\%$ , calculated from MPI-1 index after Radke and Welte (1983); and  $C_{31} 22\text{S}/(22\text{S} + 22\text{R})$  homohopane ratio approaching equilibrium, Peters et al. (2005)).

Using established procedures (Robert et al., 2016) powdered rocks were Soxhlet-extracted (9:1 DCM: MeOH; 72 h) to separate the solvent-soluble bitumen and solvent-insoluble kerogen fraction; elemental S (found to be negligible) was removed from the bitumen fraction with activated (HCl) copper (Robert et al., 2016). Column chromatography of the bitumen fraction on silica gel yielded aliphatic, aromatic and polar fractions. To further con-

\* Corresponding author at: Alfred Wegener Institute for Polar and Marine Research, Marine Geochemistry, 27568 Bremerhaven, Germany.

E-mail addresses: [h.grotheer@curtin.edu.au](mailto:h.grotheer@curtin.edu.au), [Hendrik.Grotheer@AWI.de](mailto:Hendrik.Grotheer@AWI.de) (H. Grotheer).

**Table 1**

Sample information and key compositional parameters of native sediment samples from the Hovea-3 core (Perth Basin, Western Australia) and the Toolebuc Formation (Queensland, Australia).

Sample number	Sample name	Age	TOC [wt.%]	TS [ $\mu\text{molS/g Rock}$ ]	C <sub>31</sub> 22 S/(22 S + 22R) homohopane <sup>a</sup>	MPI-1 <sup>a,b</sup>	R <sub>c</sub> <sup>c</sup>
H1	Hovea-3 1975.6m	Triassic	2.1	218.8	0.59	0.64	0.83
H2	Hovea-3 1980.05m	Triassic	0.9	n.a	0.56	0.56	0.79
H3	Hovea-3 1980.94m	Permian/Triassic	4.6	1062.5	0.57	0.55	0.78
H4	Hovea-3 1990.2m	Permian	2.1	312.5	0.58	0.58	0.80
T1	Boullia-10B 43.35m	Cretaceous	28.8	1125	0.40	0.55	0.73
T2	Jericho-11 60.78m	Cretaceous	15.6	531.3	0.38	0.50	0.70
T3	Crydon-1 101m	Cretaceous	46.2	1156.3	0.44	0.66	0.80

<sup>a</sup> Determined in bitumen extract.

<sup>b</sup> Methyl phenanthrene index after Cassani et al. (1988); calculated from base ion abundances (phenanthrene *m/z* 178; methyl phenanthrene *m/z* 192).

<sup>c</sup> Calculated vitrinite reflectance (R<sub>c</sub>); calculated from MPI-1 index after Radke and Welte (1983).

centrate OSCs, aromatic fractions were fractionated over aluminium oxide (Type 507C neutral; Fluka); using solutions of *n*-hexane:DCM (99:01 v/v), *n*-hexane:DCM (90:10 v/v) and DCM in a refined procedure outlined by Jiang et al. (2013) – the OSCs exclusively eluted in the third sub-fraction. Remnant carbonates were removed from the kerogen fraction by treatment with concentrated HCl at ~60 °C (24 h).

The kerogen (~1 g) and a DBT standard (Aldrich, 50  $\mu\text{L}$  of 100 ppm solution on 0.5 g silica gel) were individually pyrolysed using a STRATA Technology Ltd Hydropyrolyser with standard operating conditions (e.g. Grotheer et al., 2015; Robert et al., 2016) and the exclusion of a sulfide catalyst to avoid cross-reactions between sample and catalyst S. The total HyPy products (from the kerogen) were separated into polarity based fractions by column chromatography and activated copper was again used to remove any elemental S as described above.

All fractions were analysed on a HP 6890 gas chromatograph (GC) coupled to an Agilent 5975 mass selective detector (MSD). Separation was achieved on a DB-5MS capillary column (60 m  $\times$  0.25 mm i.d.  $\times$  0.25  $\mu\text{m}$ ) with He carrier gas (ultra-high purity, constant flow: 1.3 mL/min) and the following temperature program: 40 °C (2 min), then ramped to 325 °C at 3 °C/min and held for 30 min. Full scan (*m/z* 30–530) spectra were acquired with 70 eV at a scan rate of ~4 scans per second. OSC identification was based on mass spectral and GC elution position correlated to published data (e.g. Asif et al., 2009). Quantification was measured from base ion abundances (dibenzothiophene (DBT) *m/z* 184; methyl dibenzothiophenes (mDBTs) *m/z* 198) relative to an external calibration curve established with pure DBT standards.

OSC  $\delta^{34}\text{S}$  values were measured with a Thermo Neptune Plus multi-collector ICP-MS coupled to an Agilent 6890 GC inlet system (GC-ICP-MS; Greenwood et al., 2014) and are reported in permil (‰) relative to Vienna Canyon Diablo Troilite (VCDT). Analytical precision was assessed by daily analyses of a mixture of OSCs with a standard deviation better than 1.6‰.  $\delta^{34}\text{S}_{\text{OSC}}$  values reported for Hovea-3 and Toolebuc rocks represent the average of at least duplicate analyses.

The total S content and bulk  $\delta^{34}\text{S}$  of the untreated rock and the subsequently isolated kerogen fraction (following inorganic sulfur removal via Cr(II) distillation; Fossing and Jørgensen, 1989; Passier et al., 1999) were measured via combustion-isotope ratio monitoring mass spectrometry (C-irmMS) in a Thermo Flash 2000 connected to a Thermo Finnigan MAT 253 via a Thermo Conflow III interface (C-irmMS; Böttcher and Schnetger, 2004; Böttcher et al., 2006).  $\delta^{34}\text{S}$  was calibrated to the VCDT scale following Mann et al. (2009).

### 3. Results

**DBT Standard:** HyPy fully consumed the DBT with a 77  $\pm$  8 wt.% recovery in the pyrolysate, where losses are likely due to conden-

sation within the HyPy reactor or transfer line (Grotheer et al., 2015). No other reaction products were detected. The  $\delta^{34}\text{S}$  of the pure DBT standard was +5.5‰ ( $\pm$  1.1‰). Following HyPy treatment the DBT pyrolysate had a  $\delta^{34}\text{S}$  of +6.6‰ ( $\pm$  0.3‰), representing a minor enrichment (Table 2).

**Hovea-3 and Toolebuc rocks:** The Hovea-3 sedimentary rocks bitumen extracts contained very low concentration of OSCs, which principally consisted of DBT and C<sub>1</sub>–C<sub>3</sub> alkyl DBTs. The bitumen concentrations of S bound to DBT and mDBT (sum of four isomers) ranged from 0.44–0.98 nmolS/gRock and 1.81–8.19 nmolS/gRock, respectively with DBT/mDBTs ratios between 0.3 and 1.3. Much higher concentrations of OSCs (4–12 $\times$  bitumen levels; Table 2; Fig. 1) with DBT/mDBT ratios of 0.3–0.6 were generally detected following HyPy treatment of the kerogen fraction. The Toolebuc rocks had a relatively high S content, but the bitumen extracted from these rocks contained very low DBT and mDBT S concentrations (0.01–0.24 nmolS/gRock and 0.04–0.87 nmolS/gRock). HyPy treatment of the Toolebuc kerogens generated significantly higher concentrations of OSCs, as much as 3 orders of magnitude above bitumen levels (Table 2).

$\delta^{34}\text{S}$  values of DBT and mDBT were measured from all bitumen and kerogen fractions (Table 2; Fig. 2), but lower concentration of C<sub>2</sub>- and C<sub>3</sub>- DBTs prevented their  $\delta^{34}\text{S}$  analysis.  $\delta^{34}\text{S}$  values of DBT in the Hovea-3 bitumens ranged from –16.8 to –10.7‰. The  $\delta^{34}\text{S}$  values of kerogen OSCs produced by HyPy were consistently lower, with DBT up to 12.2‰ and mDBTs up to 9.4‰ lighter than their bitumen values (Table 2).  $\delta^{34}\text{S}$  of mDBTs (average of 4 isomers) were usually depleted (by up to 4‰) relatively to co-occurring DBT, which seems a common feature of the  $\delta^{34}\text{S}$  profile of methylated DBTs from oils (Greenwood et al., 2014).

$\delta^{34}\text{S}$  data from the Toolebuc sediments (Table 2) showed similar trends with DBT and mDBT from the kerogen being significantly lighter than in the bitumens (by up to 8.8‰) and mDBT values being slightly lighter (up to 3.3‰) than co-occurring DBT.

### 4. Discussion

HyPy treatment of kerogens produced much higher concentrations of OSCs than were present in the corresponding bitumen fractions. Enhanced hydrocarbon yields are typical of the HyPy treatment of carbonaceous materials (e.g. Love et al., 1998).

DBT and mDBTs from the kerogen were significantly depleted in  $^{34}\text{S}$ , with  $\delta^{34}\text{S}$  values up to 12‰ lower than their occurrence in the bitumen fraction of the rocks. This differential was much greater than the small ~1‰  $\delta^{34}\text{S}$  enrichment observed with the HyPy treatment of the DBT standard, which implied the HyPy procedure contributed minimal  $^{34}\text{S}$  fractionation.

The lower kerogen  $\delta^{34}\text{S}$  values is opposite to the common  $\delta^{13}\text{C}$  trend of heavier values from the kerogen hydrocarbon compounds compared to bitumen hydrocarbons of sedimentary rocks. The kerogen enrichment in  $^{13}\text{C}$  arises from preferential cleavage of

**Table 2**  
Quantification,  $\delta^{34}\text{S}$  values and relative abundances (DBT/mDBTs) of Soxhlet extractable (Bitumen) and HyPy released (Kerogen) OSCs.

Sample number		Kerogen S [ $\mu\text{molS/g}$ Rock]	C DBT [nmolS/g Rock]	C mDBTs [nmolS/g Rock]	DBT/ mDBT	$\delta^{34}\text{S}$ Kerogen [‰ VCDT]	$\delta^{34}\text{S}$ DBT [‰ VCDT]	SV $\pm$	$\delta^{34}\text{S}$ mDBT [‰ VCDT]	SV $\pm$	$\Delta\delta^{34}\text{S}$ DBT <sub>(Ker-Bit)</sub>	$\Delta\delta^{34}\text{S}$ mDBT <sub>(Ker-Bit)</sub>
DBT	Native						5.5	1.1				
	HyPy						6.6	0.3				
H1	Bitumen		0.71	2.1	0.34		-15.5	0.1	-18.0	1.0	-4.1	-1.8
	Kerogen	150	8.19	24.17	0.34	-28.0	-19.6	0.3	-19.8	1.1	-4.1	-1.8
H2	Bitumen		0.44	0.94	0.47		-16.8	0.3	-18.9	1.1		
	Kerogen	96.9	4.93	16.54	0.30	-33.7	-26.1	0.0	-24.6	0.0	-9.3	-5.7
H3	Bitumen		0.98	1.74	0.56		-15.6	0.8	-18.7	0.1		
	Kerogen	243.8	4.8	13.81	0.35	-34.7	-27.8	0.3	-26.7	0.8	-12.2	-8.0
H4	Bitumen		0.49	0.39	1.26		-10.7	0.4	-7.8	1.1		
	Kerogen	37.5	1.81	4.28	0.42	-38.1	-15.8	1.4	-17.2	0.8	-5.1	-9.4
T1	Bitumen		0.01	0.04	0.25		-12.1	0.3	-15.4	0.5		
	Kerogen	187.5	78.63	133.54	0.59	-30.3	-20.9	0.1	-20.3	1.0	-8.8	-4.9
T2	Bitumen		0.05	0.17	0.29		-28.4	1.6	-30.9	1.1		
	Kerogen	31.3	29.13	57.63	0.51	-28.2	-31.8	2.0	-32.5	1.2	-3.4	-1.6
T3	Bitumen		0.24	0.87	0.28		-22.5	0.1	-23.2	0.3		
	Kerogen	375	111.54	221.45	0.50	-34.5	-27.9		-29.5		-5.4	-6.3

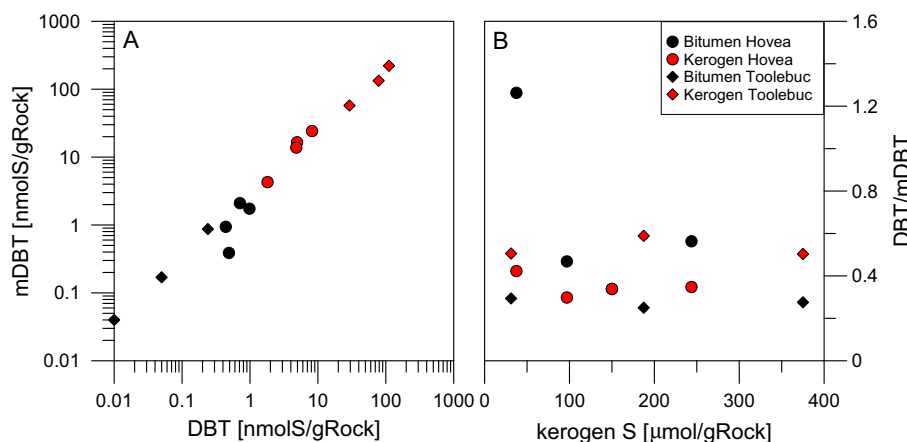


**Fig. 1.** Concentration cross-plots of (A) of bitumen (black) and kerogen (red) DBT over mDBT showing a close abundance correlation; and (B) DBT/mDBT ratio over kerogen S showed no obvious relationship between the distribution of OSCs and kerogen S concentration. (For interpretation of the references to colour in this figure legend, the reader is referred to the web version of this article.)

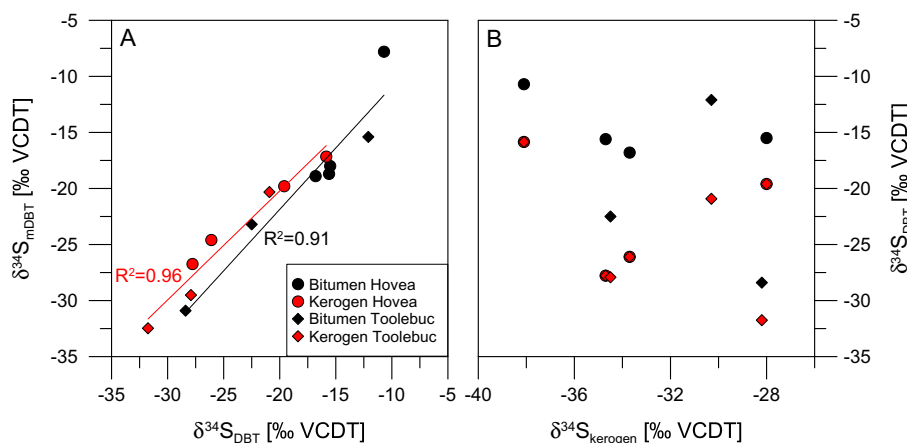


**Fig. 2.**  $\delta^{34}\text{S}$  cross-plot (A) of bitumen (black) and kerogen (red) of DBT over mDBT which showed a close isotopic correlation and implied a generic link of OSCs in each fraction, as well that kerogen bound OSCs were generally  $^{34}\text{S}$  depleted relative to bitumen OSCs; and (B)  $\delta^{34}\text{S}_{\text{DBT}}$  over bulk  $\delta^{34}\text{S}_{\text{kerogen}}$  showed no apparent isotopic relationship. (For interpretation of the references to colour in this figure legend, the reader is referred to the web version of this article.)

$^{12}\text{C}$  bonds during diagenesis and thermal cracking (e.g. Tang et al., 2000), although the respective  $\delta^{13}\text{C}$  values can also be influenced by the varied bitumen and kerogen contribution of different sources (Love et al., 1998). The  $\delta^{34}\text{S}$  differences observed in the

kerogen and bitumen fractions may similarly be due to a different representation of S-sources or sulfurisation pathways.

The OSCs in immature sediments from the Cariaco Basin formed during early diagenesis were proposed to form *via* multiple sulfurisation pathways characterised by distinct  $\delta^{34}\text{S}$  values, with two

main organic sulfurisation mechanisms supported (Raven et al., 2015):

- (i) Reaction of dissolved  $\text{HS}^-$  with OM resulting in the intramolecular addition of S. This kinetically favours incorporation of  $^{32}\text{S}$  ( $\delta^{34}\text{S}$  light organic S), and difficulties in releasing intramolecularly bound S make this a relatively irreversible reaction.
- (ii) Intermolecular addition of polysulfides ( $\text{S}_x^{2-}$ ) between different organic units. A reverse of this process could subsequently release the  $\text{S}_x$ -bridges from the organic moiety, and the equilibrium status of these reactions determines the  $\delta^{34}\text{S}$  of this organic S.

Raven et al. (2015) considered pathway ii most likely responsible for the relative  $^{34}\text{S}$  enrichment traditionally attributed to the organic incorporation of reduced S sources during diagenesis and measured in previous laboratory experiments (e.g., Amrani and Aizenshtat, 2004).

Catagenetic (i.e., temperature and pressure driven) cleavage reactions of the kerogens within the oil window maturity Hovea and Toolebuc rocks most likely contributed to their bitumen OSCs. The S of these compounds may derive from diagenetically incorporated intra- (C-S-C) or inter-molecularly (C-S<sub>x</sub>-C) bound kerogen S. S-aromatic forming reactions during diagenesis or upon maturation would favour ring-closure with the smaller  $^{32}\text{S}$  atom resulting in OSCs more depleted in  $^{34}\text{S}$  than the initial S-source. On this basis, the bitumen OSCs might be expected to be more depleted than the S-structures remaining in the kerogen fraction. Further fractionation, however, may be encountered with subsequent geologic processes such as the secondary cracking of the bitumen OSCs to form  $\text{H}_2\text{S}$ . This process would also kinetically favour the release of  $^{32}\text{S}$  enriched  $\text{H}_2\text{S}$ , such that the residual liquid phase OSCs become heavier in  $\delta^{34}\text{S}$ .

Alternatively, the bitumen fraction may subsequently incorporate or isotopically exchange with a relatively heavy S source. Raven et al. (2015) cautioned the possibility of  $\delta^{34}\text{S}$  equilibration between different (organic and inorganic) S-pools within the immature Cariaco Bay basin sediments. A previous  $\delta^{34}\text{S}$  comparison of the whole bitumen and kerogen fractions of Monterey Formation sediments also showed a trend of kerogen fractions being depleted in  $^{34}\text{S}$  relative to corresponding bitumen (Idiz et al., 1990). These authors suggested that isotopically heavy, non-reacted pore water  $\text{H}_2\text{S}$ , may have been preferentially incorporated into the asphaltene fraction of kerogen released bitumens, reflecting a varied timing and mode of organic sulfurisation and different pathways of bitumen formation. The kerogen moiety of the rock might also have continued to develop after bitumen expulsion contributing to a change in the relative abundance or  $\delta^{34}\text{S}$  nature of the main bound organic-S structures.  $\text{S}_x^{2-}$ -bridges can link organic functionalities to promote geo-polymerisation. The abundance of these S-linkages may have increased with kerogen development over geologic time and their later formation may have been from a relatively  $^{34}\text{S}$  depleted source of S or involved reactions favoring the lighter isotope. The kerogen S of these rocks may thus have evolved into a more  $^{34}\text{S}$  depleted form than from which the bitumen was earlier released. The bulk  $\delta^{34}\text{S}$  of the kerogen fraction (Table 2; Fig. 2) were generally even more depleted than the  $\delta^{34}\text{S}_{\text{OSC}}$  values measured, reflecting the presence of other isotopically lighter S-species within the kerogen matrix.

## 5. Conclusions

HyPy treatment of the kerogen fractions released significantly higher concentrations of OSCs as detected in the solvent extracta-

ble bitumen fractions. The  $\delta^{34}\text{S}$  composition of DBT and mDBTs in the HyPy produced kerogen fractions were significantly lighter (by up to 12‰) compared to their structurally free bitumen occurrence, indicating that the kerogen and bitumen of sedimentary rocks contain isotopically distinct pools of organic S. There are several possible causes of this isotopic differences including different processes, sources or timing of generation. Further  $\delta^{34}\text{S}$  evaluation of the OSCs in sedimentary OM may help to resolve the relative importance of different organic sulfurisation pathways and their contribution to hydrocarbon biomarker preservation.

## Acknowledgments

This study was conducted as part of the CSIRO Flagship Collaboration Fund Cluster for Organic Geochemistry of Mineral Systems. HG thanks CSIRO and Curtin University (scholarships) and KG thanks the ARC (DP150102235) for funding support. Geoff Chidlow, Peter Hopper and Iris Schmiedinger provided analytical support. Chris Boreham (Geoscience Australia) kindly provided the Toolebuc Formation rocks. We thank the journal reviewers (Morgan Raven and two anonymous) and Editors (D. Strapoc and E. Idiz) for their constructive advice which improved earlier versions of our study.

Associate Editor—Dariusz Strapoc

## References

- Amrani, A., Aizenshtat, Z., 2004. Mechanisms of sulfur introduction chemically controlled:  $\delta^{34}\text{S}$  imprint. *Organic Geochemistry* 35, 1319–1336.
- Amrani, A., Sessions, A.L., Adkins, J.F., 2009. Compound-specific  $\delta^{34}\text{S}$  analysis of volatile organics by coupled GC/multicollector-ICPMS. *Analytical Chemistry* 81, 9027–9034.
- Asif, M., Alexander, R., Fazeelat, T., Pierce, K., 2009. Geosynthesis of dibenzothiophene and alkyl dibenzothiophenes in crude oils and sediments by carbon catalysis. *Organic Geochemistry* 40, 895–901.
- Boreham, C.J., Powell, T.G., 1987. Sources and preservation of organic matter in the Cretaceous Toolebuc Formation, eastern Australia. *Organic Geochemistry* 11, 433–449.
- Böttcher, M.E., Hetzel, A., Brumsack, H.J., Schipper, A., 2006. Sulfur-iron-carbon geochemistry in sediments of the Demerara Rise. In: *Proceedings of the Ocean Drilling Program Scientific Results*, vol. 207, 23pp.
- Böttcher, M.E., Schnetger, B., 2004. Direct measurement of the content and isotopic composition of sulfur in black shales by means of combustion-isotope-ratio-monitoring mass spectrometry (C-irmMS). In: de Groot, P. (Ed.), *Handbook of Stable Isotope Analytical Techniques*, vol. 1. Elsevier, pp. 597–603.
- Cai, C., Li, K., Anlai, M., Zhang, C., Xu, Z., Worden, R.H., Wu, G., Zhang, B., Chen, L., 2009. Distinguishing Cambrian from Upper Ordovician source rocks: evidence from sulfur isotopes and biomarkers in the Tarim Basin. *Organic Geochemistry* 40, 755–768.
- Cassani, F., Gallango, O., Talukdar, S., Vallejos, C., Ehrmann, U., 1988. Methylphenanthrene maturity index of marine source rock extracts and crude oils from the Maracaibo Basin. *Organic Geochemistry* 13, 73–80.
- Dawson, D., Grice, K., Alexander, R., 2005. Effect of maturation on the indigenous  $\delta\text{D}$  signatures of individual hydrocarbons in sediments and crude oils from the Perth Basin (Western Australia). *Organic Geochemistry* 36, 95–104.
- Fossing, H., Jørgensen, B.B., 1989. Measurement reduction of a single-step chromium method Evaluation. *Biogeochemistry* 8, 205–222.
- Greenwood, P.F., Amrani, A., Sessions, A., Raven, M.R., Holman, A., Dror, G., Grice, K., McCulloch, M.T., Adkins, J.F., 2014. Development and initial biogeochemical applications of compound-specific sulfur isotope analysis. In: Grice, K. (Ed.), *Principles and Practice of Analytical Techniques in Geosciences*. Royal Society of Chemistry, UK, pp. 285–312.
- Grotheer, H., Robert, A.M., Greenwood, P.F., Grice, K., 2015. Stability and hydrogenation of polycyclic aromatic hydrocarbons during hydrolysis (HyPy) – relevance for high maturity organic matter. *Organic Geochemistry* 86, 45–54.
- Idiz, E.F., Tannenbaum, E., Kaplan, I.R., 1990. Pyrolysis of high-sulfur monterey kerogens. In: Orr, W.L., White, C.M. (Eds.), *Geochemistry of Sulfur in Fossil Fuels*. American Chemical Society, Washington D.C., pp. 575–591.
- Jiang, A., Zhou, P., Sun, Y., Xie, L., 2013. Rapid column chromatography separation of alkylnaphthalenes from aromatic components in sedimentary organic matter for compound specific stable isotope analysis. *Organic Geochemistry* 60, 1–8.
- Love, G.D., Snape, C.E., Carr, A.D., Houghton, R.C., 1995. Release of covalently-bound alkane biomarkers in high yields from kerogen via catalytic hydrolysis. *Organic Geochemistry* 23, 981–986.

- Love, G.D., Snape, C.E., Fallick, A.E., 1998. Differences in the mode of incorporation and biogenicity of the principal aliphatic constituents of a type I oil shale. *Organic Geochemistry* 28, 797–811.
- Mann, J.L., Vocke, R.D., Kelly, W.R., 2009. Revised  $\delta^{34}\text{S}$  reference values for IAEA sulfur isotope reference materials S-2 and S-3. *Rapid Communications in Mass Spectrometry* 23, 1116–1124.
- Passier, H.F., Bosch, H.-J., Nijenhuis, I.A., Lourens, L.J., Böttcher, M.E., Leenders, A., Damsté, J.S.S., de Lange, G.J., de Leeuw, J.W., 1999. Sulphidic Mediterranean surface waters during Pliocene sapropel formation. *Nature* 397, 146–149.
- Peters, K.E., Walters, C.C., Moldowan, J.M., 2005. *The Biomarker Guide. Biomarkers and Isotopes in Petroleum Exploration and Earth History*, vol. 2. Cambridge University Press.
- Radke, M., Welte, D.H., 1983. The methylphenanthrene index (MPI): a maturity parameter based on aromatic hydrocarbons. *Advances in Organic Geochemistry* 1981, 504–512.
- Raven, M.R., Adkins, J.F., Werne, J.P., Lyons, T.W., Sessions, A.L., 2015. Sulfur isotopic composition of individual organic compounds from Cariaco Basin sediments. *Organic Geochemistry* 80, 53–59.
- Robert, A.M., Grotheer, H., Greenwood, P.F., McCuaig, T.C., Bourdet, J., Grice, K., 2016. The hydropyrolysis (HyPy) release of hydrocarbon products from a high maturity kerogen associated with an orogenic Au deposit and their relationship to the mineral matrix. *Chemical Geology* 425, 127–144.
- Sinninghe Damste, J.S., de Leeuw, J.W., 1990. Analysis, structure and geochemical significance of organically-bound sulphur in the geosphere: state of the art and future research. *Organic Geochemistry* 16, 1077–1101.
- Tang, Y., Perry, J.K., Jenden, P.D., Schoell, M., 2000. Mathematical modeling of stable carbon isotope ratios in natural gases. *Geochimica et Cosmochimica Acta* 64, 2673–2687.
- Thomas, B.M., Willink, R.J., Grice, K., Twitchett, R.J., Purcell, R.R., Archbold, N.W., George, A.D., Tye, S., Alexander, R., Foster, C.B., Barber, C.J., 2004. Unique marine Permian-Triassic boundary section from Western Australia. *Australian Journal of Earth Sciences* 51, 423–430.
- Woltering, M., Tulipani, S., Boreham, C.J., Walshe, J., Schwark, L., Grice, K., 2016. Simultaneous quantitative analysis of Ni, VO, Cu, Zn and Mn geoporphyrins by liquid chromatography-high resolution multistage mass spectrometry: method development and validation. *Chemical Geology* 441, 81–91.